Research Article

Pulmonary Circulation

Biventricular diastolic dysfunction, thrombocytopenia, and red blood cell macrocytosis in experimental pulmonary arterial hypertension

Ji Young Lee[1,2,3,4,*], Karen A. Fagan[2,3,4,5], Chun Zhou[1,4], Lynn Batten[1,2,4,6], Michael V. Cohen[1,2,4,7] and Troy Stevens[1,2,4,*]

[1]Department of Physiology and Cell Biology, University of South Alabama, Mobile, AL, USA; [2]Department of Internal Medicine, University of South Alabama, Mobile, AL, USA; [3]Division of Pulmonary and Critical Care Medicine, University of South Alabama, Mobile, AL, USA; [4]Center for Lung Biology, University of South Alabama, Mobile, AL, USA; [5]Department of Pharmacology, University of South Alabama, Mobile, AL, USA; [6]Department of Pediatrics, University of South Alabama, Mobile, AL, USA; [7]Division of Cardiology, University of South Alabama, Mobile, AL, USA

Abstract

Pulmonary arterial hypertension is a fatal disease, where death is associated with right heart failure and reduced cardiorespiratory reserve. The Sugen 5416, hypoxia and normoxia Fischer rat model mimics human pulmonary arterial hypertension, although the cause(s) of death remains incompletely understood. Here, we hypothesized that these animals develop biventricular diastolic dysfunction that contributes to tissue hypoperfusion coincident with severe pulmonary arterial hypertension. We performed comprehensive echocardiographic and hematologic assessments. Serial echocardiogram at 3–5 weeks was performed followed by blood sampling via aortic or cardiac puncture. Echocardiogram revealed pulmonary arterial hypertension in pulmonary artery Doppler waves, including notched wave envelopes, and decreased pulmonary artery acceleration time/pulmonary artery ejection time ratio and right ventricular outflow tract velocity time integral. Impaired right ventricular systolic function, assessed by decreased tricuspid annular plane systolic excursion and tricuspid tissue Doppler systolic positive wave velocity, was observed in pulmonary arterial hypertension. Tricuspid and mitral pulsed wave and tissue Doppler findings suggested biventricular diastolic dysfunction, with dynamic changes in early and late diastolic filling waves, their fusion patterns, and a decrease in e' velocity. Heart rate and ejection fraction did not change, but cardiac output, stroke volume, and end-diastolic volume were decreased, and inferior vena cava respiratory variation was decreased. Blood electrolyte values were suggestive of intravascular volume expansion early in the disease followed by volume contraction and tissue hypoperfusion in the latter stages of disease. Complete blood count showed thrombocytopenia and non-anemic macrocytosis with reticulocytosis and an increase in red blood cell distribution width. Thus, pulmonary, cardiac, and hematological findings in Fischer animals with pulmonary arterial hypertension are characteristic of humans and provide an insightful experimental platform to resolve mechanisms of disease progression.

Keywords

Sugen 5416, bone marrow, thrombocytopenia, mean corpuscular volume (MCV), red cell distribution width (RDW)

Date received: 6 August 2019; accepted: 1 February 2020

Pulmonary Circulation 2020; 10(2) 1–12
DOI: 10.1177/2045894020908787

Introduction

Pulmonary arterial hypertension (PAH) is a progressive and fatal disease.[1] Due to the nonspecific clinical presentations and heterogeneous patient phenotypes,[2] timely diagnosis is

*These authors contributed equally to this work.

Corresponding author:
Troy Stevens, Department of Physiology and Cell Biology, Center for Lung Biology, College of Medicine, University of South Alabama, Mobile, AL 36688, USA.
Email: tstevens@southalabama.edu

challenging and initiation of therapy is often delayed.[3] Despite rapid advancement in understanding the pathophysiology of PAH, and despite the development of targeted therapies that increase life longevity,[4] the causes of death among PAH patients remain elusive. The direct cause of death in PAH patients was thought to be mainly progression of right heart failure.[5] However, in a cross-sectional study addressing the cause of death of PAH patients, respiratory disease, pulmonary embolism, sepsis, acute renal failure, and other cardiovascular disease accounted for 44% of the deaths.[6] Furthermore, multiple non-PAH specific factors, such as renal failure[7] and thrombocytopenia,[8] independently predict PAH mortality. Recently, unbiased phenome-wide association studies revealed that among 1364 coded medical conditions, red cell distribution width (RDW) and pulmonary hypertension have the strongest association.[9] Although the implications of this finding remain to be determined, they suggest that PAH pathophysiology is not lung-specific, but rather, involves multiple organ systems.

Animal models can help to reveal cause-and-effect relationships of associated diseases when they closely mimic the human condition. A rat PAH model induced by a single injection of Sugen 5416 followed by three weeks of exposure to 10% oxygen and then 3–10 weeks of normoxia, in addition to severe PAH development, uniquely reproduces occlusive vasculopathy of pulmonary arteries, which is not observed in more classic rat PAH models such as the chronic hypoxia and monocrotaline models.[10–12] Using the Sugen/hypoxia model, we discovered that PAH progresses to death in Fischer rats, a finding that is atypical among most rodent species.[13] Subsequently, Jiang and colleagues revealed significant differences in disease severity and mortality between rat strains and colonies in this model; in their work, mortality in Fischer rats and selective Sprague-Dawley species was attributed to acute right heart failure.[14] These findings emphasize the contribution of genetic factors to PAH susceptibility, as heterogeneous populations of rats may mirror human PAH populations with variable disease courses. However, examining the Fischer Sugen/hypoxia model with greater emphasis on multiple organ systems may add insight into the complex physiologic milieu that contributes to death in PAH, and in doing so, identify unique subpopulations of patients best represented for translational therapies.

In our previous study, we demonstrated that Sugen, hypoxia, and normoxia exposure (Sugen/hypoxia PAH model) induces severe PAH in Fischer 344 rats, demonstrated by right heart catheterization, echocardiogram, and histopathologic examinations.[13,15] Interesting questions left unanswered from that study were why PAH animals are susceptible to sudden death, and whether there is accompanying platelet and red blood cell changes in the setting of hypoxia and occlusive vasculopathy. Here, we hypothesized that PAH rats develop biventricular dysfunction leading to global tissue hypoperfusion, thrombocytopenia, and red blood cell macrocytosis. To test this hypothesis, we performed comprehensive echocardiographic assessments and blood analysis.

Materials and methods

Rat pulmonary hypertension models

All experimental procedures were performed in accordance with current provisions of the U.S. Animal Welfare Act and were approved by the University of South Alabama Institutional Animal Care and Use Committee. Male Fischer rats weighing approximately 200 g were used. PAH was induced by a single subcutaneous injection of 20 mg/kg Sugen 5416 (Semaxanib; MedKoo Biosciences, Chapel Hill, NC) followed by exposure to three weeks of normobaric hypoxia (10% O_2) and then re-exposure to normoxia (21% O_2) for a total of three to five weeks.[15] Hereafter, this model is referred to as Fischer experimental PAH. Age-matched animals bred in normoxia for three– to five weeks without Sugen 5416 injection or hypoxia exposure were used for control group for all experiments. Exposure to hypoxia for three weeks without Sugen 5416 injection was used as a ''hypoxia only'' control group for hematologic tests.

Echocardiography

A Vevo 3100 (VisualSonics, Toronto, ON, Canada) with a 30 MHz transducer (MX550D) was used at baseline and three, four, and five weeks after Sugen, hypoxia, and normoxia exposure to evaluate the progression of cardiac dysfunction. Rats were anesthetized but kept spontaneously breathing using isoflurane 1.5% (titrated as needed) in a 1:1 O_2–air admixture. Heart rate, electrocardiogram, and respiration were continuously recorded using the sensor-embedded exam pad. To minimize potential cardiovascular stress induced by anesthesia, all measurements were completed within 20 min for each animal. From parasternal long axis view, M-mode was used to obtain left ventricular ejection fraction, stroke volume, and cardiac output. Left ventricular ejection fraction was calculated using modified Quinones method. From the parasternal short axis view at the pulmonary artery level, pulmonary artery acceleration time (PAAT)/pulmonary artery ejection time (PAET) ratio and right ventricular outflow tract (RVOT) velocity time integral (VTI) of pulmonary arterial flow were measured using pulsed wave Doppler. Apical four-chamber view was used to obtain M-mode tricuspid annular plane systolic excursion (TAPSE), mitral and tricuspid pulsed wave Doppler early (E) and late (A) filling waves, and tissue Doppler early diastolic (e'), atrial (a'), and systolic positive (S') wave velocities. In subcostal longitudinal inferior vena cava (IVC) view, minimal and maximum diameters of IVC at the hepatic venous inflow level were obtained.

Image acquisition was performed by one operator, and image analysis was performed by two examiners with cardiologist consultation following the American Society of Echocardiography guidelines.[16–18]

Blood sampling and analysis

Blood was sampled from the left ventricle immediately after the final echocardiogram at three weeks for hypoxia control and five weeks for Sugen/hypoxia animals by aortic or cardiac puncture under isoflurane anesthesia. Complete blood count and serum chemistry analysis were performed at the University of South Alabama Children's and Women's hospital laboratory.

Statistics

Two-way ANOVA, Student's *t*-tests, and Bonferroni post hoc correction and Chi-square tests were used, as appropriate. Significance was denoted as $P < 0.05$.

Results

PAH induces characteristic flow pattern changes in the pulmonary artery

To confirm the development of PAH, we performed pulsed wave Doppler on pulmonary arterial flow using the short axis view (Fig. 1a). After Sugen 5416, hypoxia and normoxia exposure, there were characteristic notch pattern changes in the flow velocity envelope (Fig. 1b) and decreases in the PAAT/PAET ratio (Fig. 1c) and RVOT VTI (Fig. 1d). The findings are consistent with those from previous studies in which we also measured concomitantly elevated pulmonary artery pressure by right heart catheterization and echocardiogram.[13,19] Thus, severe PAH was confirmed within three weeks of Sugen and hypoxia treatment.

PAH induces right ventricular systolic dysfunction

During PAH development, the right ventricle increases its mass and contractility to overcome increased afterload.

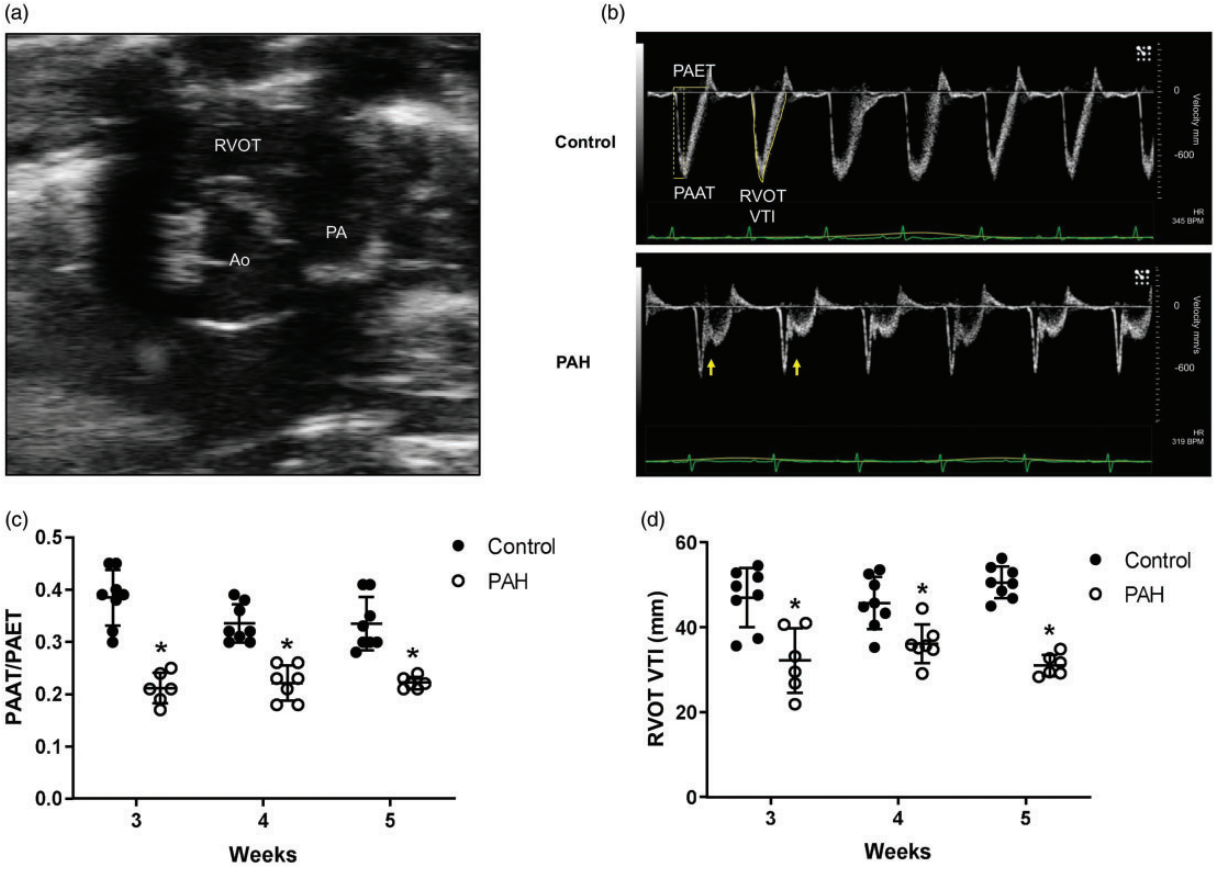

Fig. 1. PAH induces characteristic notch pattern changes and decreases PAAT/PAET ratio and RVOT VTI in pulmonary artery flow. (a) Echocardiographic evidence of PAH was assessed on the short axis view at the level of the aortic valves. Pulsed wave Doppler assessment of pulmonary artery flow shows (b) characteristic notch pattern changes (arrow) and (c) decreased PAAT/PAET ratio and (d) RVOT VTI in Fischer rats exposed to Sugen 5416, hypoxia, and normoxia.

Notes: Please note the change in Y-axis scale among images.

*Significant difference ($P < 0.05$) from Control. $n = 8$ control and 6–7 PAH animals.

Ao: aorta; RVOT: right ventricular outflow tract; PA: pulmonary artery; PAET: pulmonary artery ejection time; PAAT: pulmonary artery acceleration time; VTI: velocity time integral; PAH: pulmonary arterial hypertension.

As pulmonary arterial pressure further increases, the right ventricle dilates and its systolic function is compromised.[20] In this cohort, PAH animals developed right ventricular dilatation and septal flattening with paradoxical movements (Fig. 2a and b and supplemental movies S1 (https://figshare.com/articles/Supplemental_movie_S1/7949504), i.e. control, and S2 (https://figshare.com/articles/Supplemental_movie_S2/7949528), i.e. PAH). To assess the impact of PAH on the right heart function over time, we assessed TAPSE and S' velocity of the tricuspid annulus, two well-validated parameters of right ventricular systolic function, at three, four, and five weeks. There were significant decreases in both TAPSE (Fig. 2c and d) and tricuspid S' velocity (Fig. 2e and f) in PAH throughout the time course. The finding suggests that maximal development of right ventricular systolic dysfunction is at, or earlier than, three weeks in the Fischer experimental PAH model.

PAH induces evolving right ventricular diastolic dysfunction

Right ventricular diastolic dysfunction complicates clinical management of the PAH patient. When right ventricular relaxation is impaired, a modest degree of tachycardia can

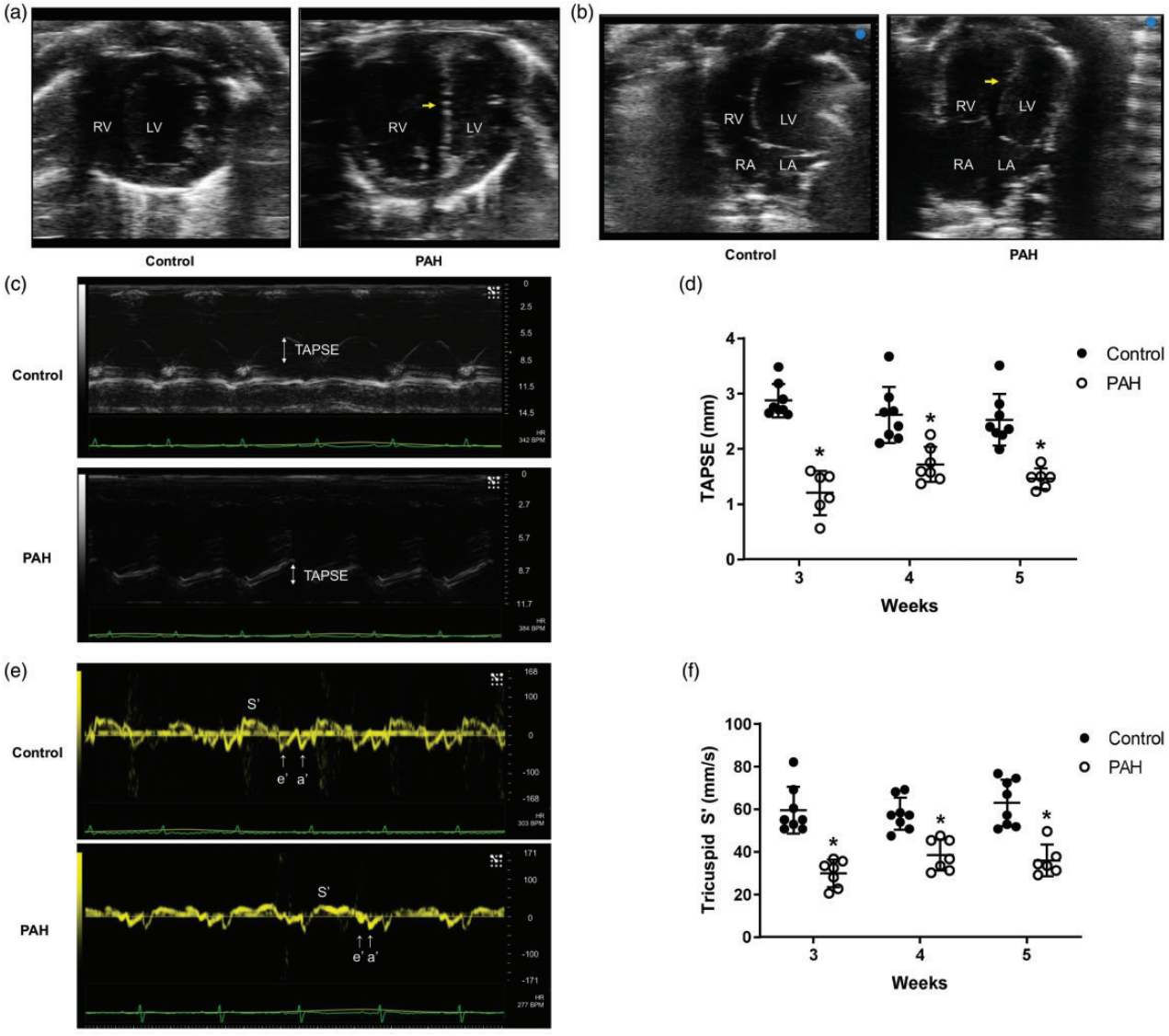

Fig. 2. PAH decreases TAPSE and S' velocity. PAH-induced RV dilatation and interventricular septal flattening (arrows) is demonstrated (a) in the short axis view at the level of the mid-ventricular level and (b) in the apical four chamber view. To assess right ventricular systolic function, M-mode of right lateral ventricular wall and tissue Doppler imaging on lateral tricuspid annulus were performed on the apical four chamber view. PAH rats developed right ventricular systolic dysfunction indicated by decreased (c and d) TAPSE and (e and f) lateral tricuspid annulus tissue S' velocity. Please note the change in Y-axis scale among images.
*Significant difference ($P < 0.05$) from control. $n = 8$ control and 6–7 PAH animals.
RV: right ventricle; LV: left ventricle; RA: right atrium; LA: left atrium; TAPSE: tricuspid annular plane systolic excursion; PAH: pulmonary arterial hypertension.

trigger sudden circulatory collapse due to insufficient right ventricular filling, subsequently causing a rapid decrease in left ventricular preload and cardiac output.[21] To assess right ventricular diastolic function, we analyzed tricuspid inflow patterns and tissue Doppler imaging of tricuspid lateral annulus over the course of three to five weeks. Compared to control, where E and A waves were clearly distinguishable except in one animal, there was a higher percentage of subjects that developed EA fusion waves, reaching 100% by five weeks, in PAH (Fig. 3a and b).

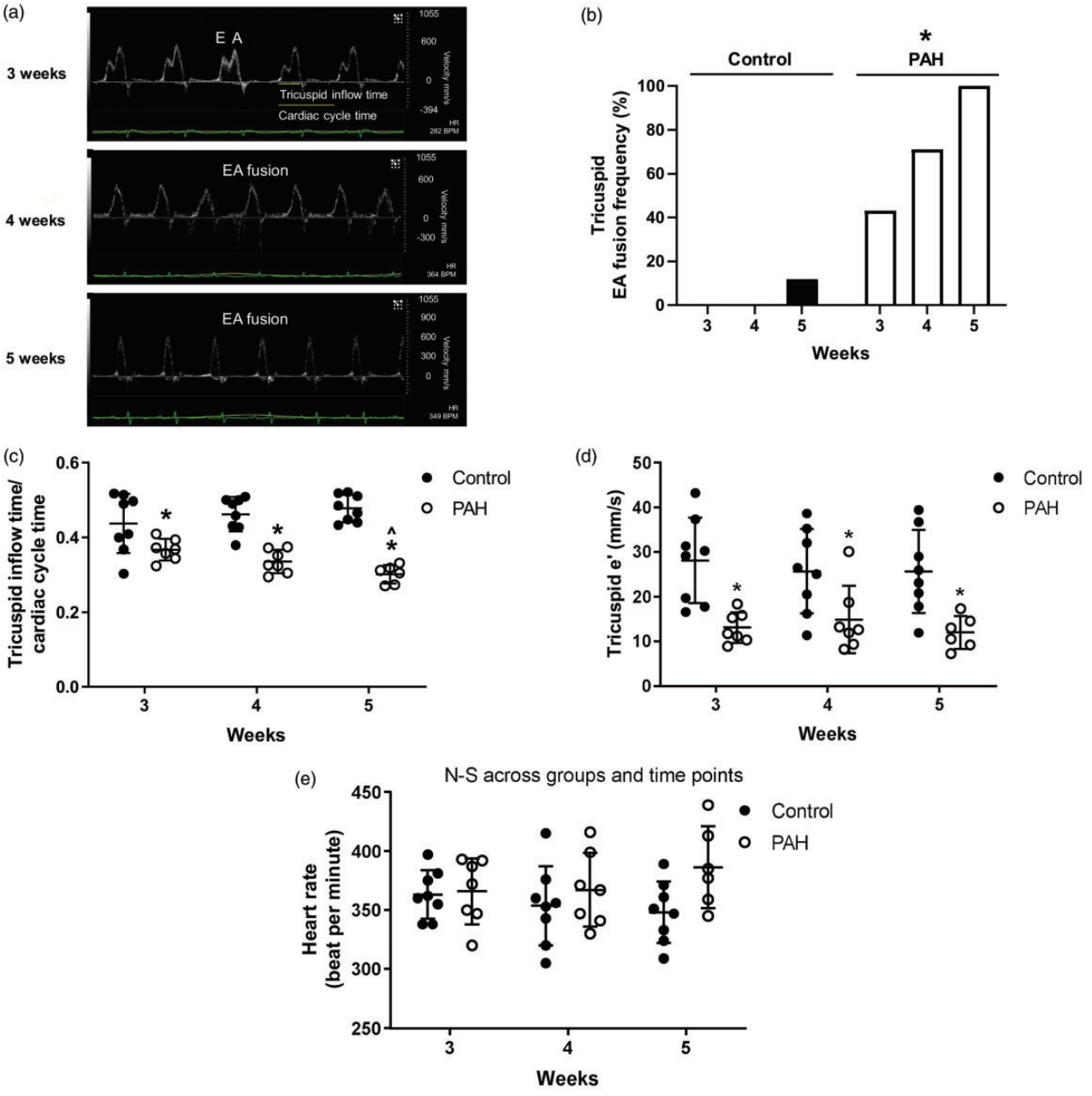

Fig. 3. PAH increases tricuspid E and A wave fusion, decreases tricuspid inflow time to cardiac cycle time ratio, and e' velocity. To assess right ventricular diastolic function, tricuspid pulsed wave Doppler and lateral tricuspid annulus tissue Doppler imaging was performed on the apical four chamber view along with continuous heart rate monitoring. PAH rats developed evolving right ventricular diastolic dysfunction indicated by (a and b) increased frequency of E and A wave fusion (a and c) decreasing tricuspid inflow time to cardiac cycle time ratio over time, and (d) decreased e' velocity (e) without changes in the heart rate.

Note: Please note the change in Y-axis scale among images.

*Significant difference ($P < 0.05$) from control.

^Significant difference ($P < 0.05$) from control three weeks.

$n = 8$ control and 6–7 PAH animals.

PAH: pulmonary arterial hypertension.

Going with this trend, tricuspid inflow time to cardiac cycle time ratio was lower in PAH, and lower in five weeks compared to three weeks among PAH subjects (Fig. 3a and c). Tricuspid tissue e' velocity was decreased in PAH (Figs. 2d and 3d). There was no statistically significant change in the heart rate throughout the time course (Fig. 3e). The findings suggest evolving right ventricular diastolic dysfunction in PAH.

PAH induces left ventricular diastolic dysfunction with preserved ejection fraction

Most PAH studies in animal models mainly focus on assessing right heart function. However, since right and left ventricles do not contract separately, their function should be inter-dependent in nature.[22] Therefore, we sought to determine how left ventricular function is affected by the right heart as PAH and right ventricular dysfunction progress. We first assessed left ventricular ejection fraction. There was no change in left ventricular ejection fraction between control and PAH suggesting preserved left ventricular systolic function (Fig. 4a and b). To assess left ventricular diastolic function, we analyzed mitral inflow patterns and tissue Doppler imaging of the mitral medial annulus over the course of three to five weeks. Similar to tricuspid inflow patterns, there was a higher percentage of E and A wave fusion (Fig. 4c and d) and decreased mitral inflow time to cardiac cycle time in PAH (Fig. 4c and e). However, unlike tricuspid inflow time to cardiac cycle time ratio, which further decreased from three weeks to five weeks, mitral inflow time to cardiac cycle time ratio did not change over time in PAH. Mitral tissue e' velocity was decreased in PAH (Fig. 4f and g). The findings suggest left ventricular diastolic dysfunction with preserved systolic function in PAH.

PAH decreases cardiac output and circulating intravascular volume

To assess the impact of biventricular diastolic failure on systemic circulatory status, we estimated cardiac output, stroke volume, and end-diastolic volume and measured IVC respiratory variation. Consistent with our previous report,[13,15] cardiac output (Fig. 5a), stroke volume (Fig. 5b), and left ventricular end-diastolic volume (Fig. 5c) were decreased in PAH. Minimal IVC diameter was increased toward four weeks, and then normalized at five weeks (Fig. 5d and e). There was no difference in maximal IVC diameter between groups throughout the time points (data not shown). IVC respiratory variation, a surrogate for right atrial pressure and fluid responsiveness,[23] was decreased at four weeks then normalized at five weeks (Fig. 5f). The findings may indicate early venous congestion that resolves over time as total effective intravascular volume decreases towards five weeks.

PAH induces biochemical features of volume contraction and tissue hypoperfusion

To further evaluate total body fluid status and its effects on global tissue perfusion, we analyzed blood chemistry panels at five weeks. In PAH, there was increased sodium, potassium, and chloride (Table 1). Bicarbonate was decreased and anion gap and lactate were increased, suggesting high anion gap metabolic acidosis. Serum osmolality, blood urea nitrogen, and creatinine were elevated in PAH, indicating dehydration. Although the aspartate aminotransferase increase may be non-specific, a mild degree of hepatic injury cannot be excluded. Overall, these findings are suggestive of volume contraction, tissue hypoperfusion, and potential nonspecific renal and/or hepatic injuries.

PAH induces thrombocytopenia, red blood cell macrocytosis, and increased red blood cell distribution width

Previous studies illustrate that there is a heterogeneous pattern of platelet and red blood cell counts/size in PAH patients, but among these studies, thrombocytopenia and red blood cell distribution width portends poor outcomes.[9,24] To identify clinically relevant platelet and red blood cell changes in Fischer experimental PAH, we performed complete blood count analysis at five weeks. Interestingly, PAH induced thrombocytopenia, with a 36% decrease in mean platelet counts compared to control (Table 2). While there was no change in red blood cell counts, hemoglobin, and hematocrit, reticulocytes were increased in PAH. The findings may suggest concomitant increase in production and destruction of red blood cells, although further confirmatory workups are needed. Mean corpuscular volume (MCV) and mean corpuscular hemoglobin (MCH) were increased and mean corpuscular hemoglobin concentration was decreased. The findings indicate increased immature red blood cells which typically possess high cell volume. Additionally, the indices of cell size variability, red blood cell distribution width-standard deviation (RDW-SD), and red blood cell distribution width-coefficient of variation (RDW-CV) were increased, reflecting increased number of immature cells with variable cell sizes. Together, the findings suggest the Fischer experimental PAH model induces thrombocytopenia, red blood cell macrocytosis, and rapid red blood cell turnover. In contrast to PAH, three weeks of hypoxia exposure, without Sugen, induced remarkable increases in red blood cells, hemoglobin, and hematocrit without significant changes in reticulocyte count. Similar to the PAH group, MCV, MCH, RDW-SD, and RDW-CV were all increased. Interestingly, white blood cell count was significantly decreased in the hypoxia group. Whether this decrease in white blood cell count indicates bone marrow exhaustion due to polycythemia is unclear. These results indicate that Fischer rats fully develop

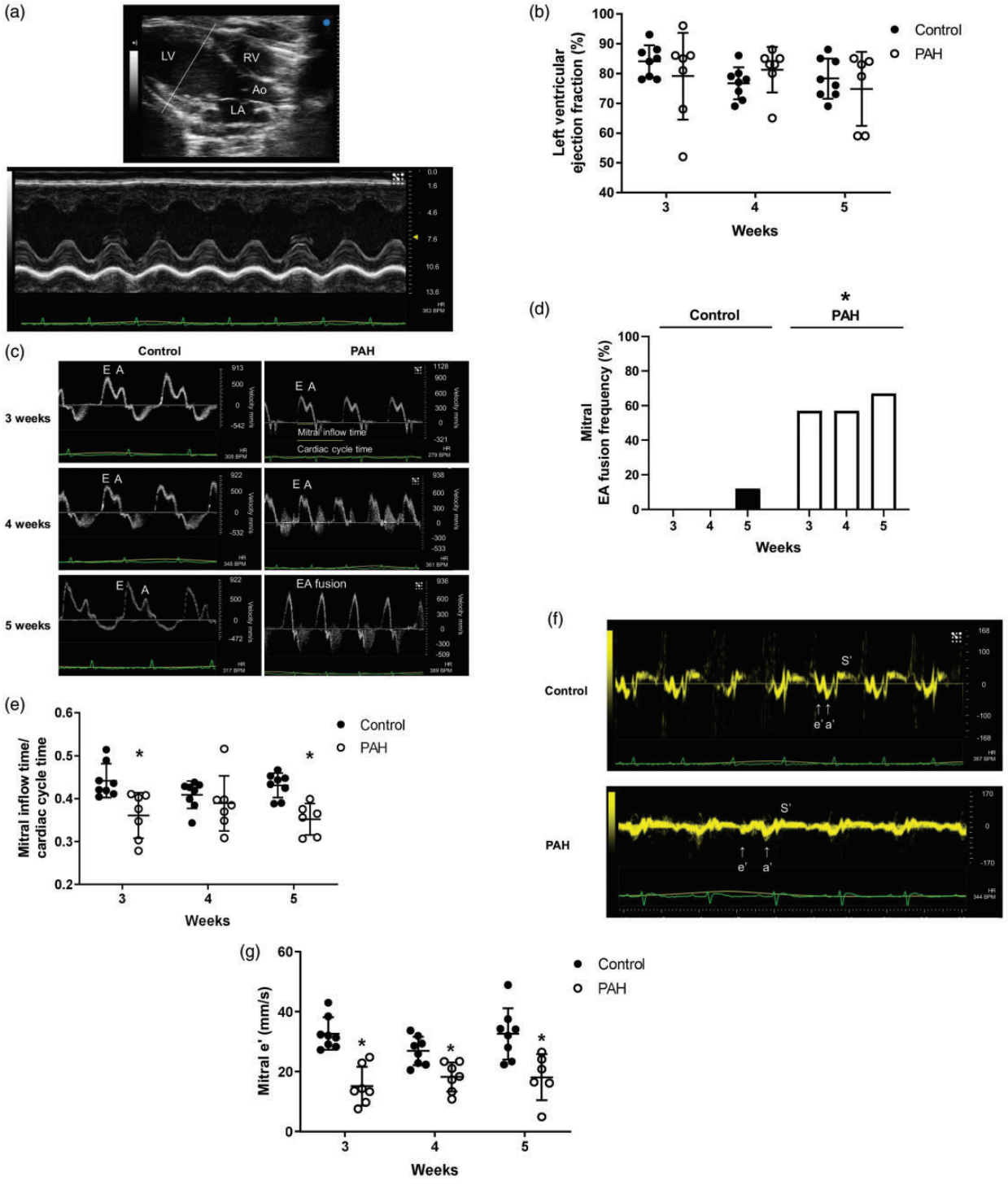

Fig. 4. PAH preserves ejection fraction but increases E and A fusion, decreases mitral inflow time to cardiac cycle time ratio, and decreases e' velocity. To assess left ventricular systolic and diastolic function M-mode of left ventricle, pulsed wave Doppler of mitral inflow and tissue Doppler of medial mitral annulus were performed on the apical four chamber view. (a and b) Left ventricular ejection fraction was preserved in PAH. (c and d) There was a higher percentage of E and A wave fusion and (c and e) decreased mitral inflow time to cardiac cycle time ratio in mitral inflow. (f and g) e' velocity was significantly low in PAH.

Note: Please note the change in Y-axis scale among images.

*Significant difference ($P < 0.05$) from control.

$n = 8$ control and 6–7 PAH animals.

LV: left ventricle; RV: right ventricle; Ao: aorta; RA: right atrium; LA: left atrium; PAH: pulmonary arterial hypertension.

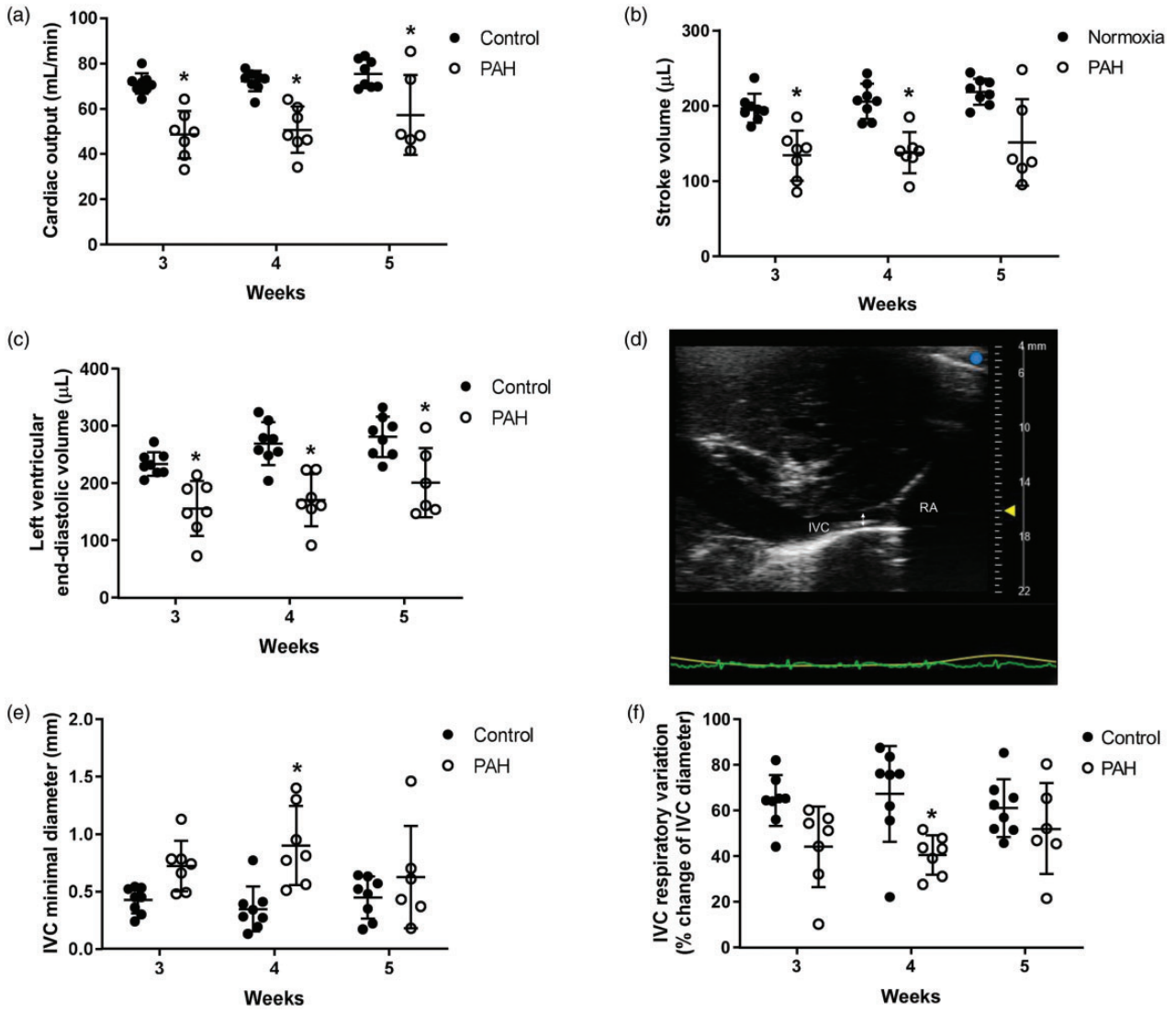

Fig. 5. PAH decreases cardiac output, stroke volume, and left ventricular end-diastolic volume and temporarily decreases IVC respiratory variation at four weeks. To assess overall intravascular volume status, cardiac output and left ventricular end-diastolic volume were estimated from M-mode measurements of left ventricle on the parasternal long axis view, and IVC diameter and respiratory variation were measured on the subcostal longitudinal IVC view. PAH decreased (a) cardiac output at three to five weeks, (b) stroke volume at three and four weeks, and (c) left ventricular end-diastolic volume at three to five weeks. (d and e) Minimal IVC diameters were increased and (f) IVC respiratory variation was decreased at four weeks indicating relatively increased right atrial pressure.
*Significant difference ($P < 0.05$) from control.
$n = 8$ control and 6–7 PAH animals.
IVC: inferior vena cava; RA: right atrium; PAH: pulmonary arterial hypertension.

secondary polycythemia in response to three weeks of hypoxia exposure.

Discussion

In this study, we performed comprehensive echocardiographic and hematologic assessments over three to five weeks on Fischer rats with severe experimental PAH. This time frame represents the typical time points when severe PAH develops but death is yet to occur; a majority of animals die between six and eight weeks.[13,14] We report three major findings, that Fischer experimental PAH induces: (1) biventricular diastolic dysfunction; (2) thrombocytopenia; and (3) red blood cell macrocytosis.

Studies on diastolic dysfunction in PAH are relatively limited. When considering the right ventricle, the association between diastolic dysfunction and PAH severity has been described and is thought to be due to myocardial hypertrophy, fibrosis, and sarcomere stiffening.[25,26] Neto-Neves et al. has recently shown right ventricular diastolic dysfunction in the Sugen/hypoxia Sprague-Dawley PAH model, using an ex vivo isolated perfused heart preparation (Langendorff

Table 1. Comprehensive metabolic panel.

Variables	Control ($N=11$)	PAH ($N=14$)	P value
Sodium (mmol/L)	137.6 (±1.5)	139.9 (±2.36)	**0.01**
Potassium (mmol/L)	4.14 (±0.42)	5.57 (±1.04)	**0.0002**
Chloride (mmol/L)	99.64 (±0.81)	102.9 (±2.30)	**0.0002**
Bicarbonate (mmol/L)	26.45 (±1.29)	23.07 (±3.03)	**0.002**
Anion gap (mmol/L)	15.68 (±0.83)	19.84 (±4.11)	**0.004**
Lactate (mmol/L)	1.46 (±0.41) (N = 6)	3.75 (±3.85) (N = 12)	**0.03**
Glucose (mg/dL)	284.8 (±79.66)	281.9 (±63.19)	0.92
Calculated osmolality (mOsm/kg)	297.9 (±4.48)	304.7 (±3.81)	**0.0004**
Calcium (mg/dL)	10.93 (±0.26)	10.67 (±0.50)	0.14
Blood urea nitrogen (mg/dL)	19.0 (±4.03)	25.93 (±4.54)	**0.0005**
Creatinine (mg/dL)	0.35 (±0.02)	0.41 (±0.07)	**0.01**
Aspartate aminotransferase (U/L)	72.0 (±14.94)	102.1 (±25.13)	**0.002**
Alanine transaminase (U/L)	48.27 (±6.02)	60.07 (±21.61)	0.09
Albumin (g/dL)	0.99 (±0.05)	0.98 (±0.06)	0.59
Total protein (g/dL)	6.2 (±0.21)	6.01 (±0.30)	0.1
Total bilirubin (mg/dL)	0.07 (±0.05)	0.1429 (±0.05)	**0.002**
Alkaline phosphatase (U/L)	264.1 (±49.86)	267.5 (±33.42)	0.84

Notes: Each value represents mean ± SD. P values were calculated compared to control group. Bolded values are significantly different from control ($P<0.05$).

Table 2. Complete blood count.

Variables	Control ($N=9$)	PAH ($N=7$)	P value	Hypoxia ($N=6$)	P value
WBC (10^6/4)	3.9 (±0.69)	4.23 (±1.21)	0.73	1.99 (±0.53)	**0.0012**
RBC (10^6/4)	8.33 (±0.18)	7.86 (±0.88)	0.21	10.76 (±0.30)	<**0.0001**
Hemoglobin (g/dL)	14.63 (±0.34)	14.81 (±1.88)	0.94	21.85 (±0.39)	<**0.0001**
Hematocrit (%)	42.53 (±1.14)	44.56 (±5.59)	0.45	63.17 (±1.05)	<**0.0001**
MCV (fL)	51.06 (±0.84)	56.69 (±1.79)	<0.0001	58.73 (±2.03)	<**0.0001**
MCH (pg)	17.57 (±0.2)	18.81 (±0.32)	<0.0001	20.33 (±0.56)	<**0.0001**
MCHC (pg)	34.42 (±0.29)	33.26 (±1.28)	**0.02**	34.58 (±0.48)	0.92
Platelet (10^3/4)	528.4 (±93.08)	336.7 (±110)	**0.002**	362.2 (±63.66)	**0.01**
RDW-SD (fL)	21.68 (±1.43)	31.7 (±5.22)	**0.0003**	39.33 (±5.09)	<**0.0001**
RDW-CV (%)	12.87 (±0.97)	17.74 (±2.81)	**0.0001**	21.18 (±0.61)	<**0.0001**
Reticulocytes (%)	3.93 (±0.66)	12.46 (±3.33)	<0.0001	4.86 (±0.42)	0.61
NRBC (/100WBC)	0.21 (±0.31)	5.69 (±9.14)	0.14	0.1 (±0.03)	0.12

Notes: Each value represents mean ± SD. P values were calculated compared to control group. Bolded values are significantly different from control ($P<0.05$). WBC: white blood cell; RBC: red blood cell; MCV: mean corpuscular volume; MCH: mean corpuscular hemoglobin; MCHC: mean corpuscular hemoglobin concentration; NRBC: nucleated RBC; RDW-SD: red blood cell distribution width-standard deviation; RDW-CV: red blood cell distribution-coefficient of variation.

preparation).[27] To our knowledge, no study has documented echocardiographic evidence of right diastolic dysfunction in the Sugen/hypoxia PAH model. In our study, decreased e' velocity represented a consistent echocardiographic sign of diastolic dysfunction in the right ventricle. In addition, diastolic parameters such as tricuspid EA fusion frequency and tricuspid inflow time to cardiac cycle time ratio dynamically evolved over time. This finding suggests that right ventricular diastolic dysfunction may help distinguish severity of PAH and can be useful in monitoring the efficacy of therapeutic interventions.

In addition to right ventricular diastolic dysfunction, we found evidence for left ventricular diastolic dysfunction in this model. Left ventricular dysfunction has been documented in both pulmonary hypertension due to left heart failure and in PAH.[20,28] In the former example, elevated left atrial pressure elicits remodeling of the pulmonary veins and the microcirculation, leading to elevated pulmonary artery and ultimately right ventricular pressures. This vascular progression culminates in a combined post- and pre-capillary pulmonary hypertension, where the cause of pulmonary hypertension is left ventricular failure that can

occur with or without preserved ejection fraction. In contrast to this cause of pulmonary hypertension, PAH with severe right ventricular remodeling leads to ventricular interdependence causing impaired left ventricular filling[29,30] and/or coexisting cardiomyopathy.[31] Diastolic dysfunction can occur even when PAH severity is mild.[32] While PAH initiates left ventricular diastolic dysfunction in this case, the resulting elevations in left atrial pressure can subsequently lead to remodeling of the pulmonary veins and microcirculation.[33] We have recently found elevated post-capillary resistance in the Fischer PAH model.[34] Future studies will be required to assess the relevance of left ventricular diastolic dysfunction to remodeling of the pulmonary veins in this model. Nonetheless, it is clear that the cause of left ventricular dysfunction in the Sugen/hypoxia Fischer PAH model is the pre-capillary vasculopathy; this model mimics human pre-capillary PAH that progresses into late-term biventricular failure with post-capillary involvement.

Fluid management in critically ill PAH patients with right heart failure is extremely challenging.[21] Minimal changes in intravascular volume can quickly overwhelm the poorly compliant right heart and result in sudden circulatory collapse. Despite its clinical relevance, fluid status is rarely reported in experimental cardiac disease models. A study with the aorta-to-vena cava fistula heart failure rat model demonstrated water retention and hyponatremia 20 days after surgery,[35] and another study using the coronary artery ligation heart failure rat model showed hyponatremia and heart weight increase three weeks postoperatively,[36] both suggesting ''fluid retention'' as a consequence of heart failure. As there is no single tool that can absolutely determine intravascular volume status,[37] we combined evidence from echocardiogram and serum chemistry panels. Over the course of three to five weeks, biventricular diastolic failure, respiratory variation of IVC nadiring at four weeks, and upward trending of the heart rate in the setting of serologic evidence of tissue hypoperfusion at five weeks, altogether suggests initial (3–4 weeks) venous congestion followed by later (five weeks) intravascular volume contraction. Although the mechanisms leading to dehydration in our PAH animals is unclear, we speculate that the degree of cardiovascular dysfunction may be severe enough to limit the activity and fluid intake of the PAH animals to ultimately result in failure to thrive. Notably, our late-stage PAH animals are extremely vulnerable to external stimuli, such as cage changes or anesthesia causing sudden death, the phenomenon similar to human PAH patients being at high risk for surgery. The findings emphasize the importance of careful systemic fluid status analysis in interpreting cardiovascular experimental models.

Thrombocytopenia predicts mortality among pulmonary hypertension of all groups,[24] and the same is true when PAH populations are considered separately.[8] Furthermore, there has been a report indicating increased platelet activation in PAH patients when mean platelet volume was used as a marker of platelet activation.[38] However, whether platelets actively drive vascular injury and inflammation or are consumed during PAH disease progression is still debatable,[39] and no randomized controlled trial supports antiplatelet therapies. Endothelial dysfunction in PAH has been well-described, and platelets are mediators of major drug target pathways including nitric oxide, prostacyclin, and endothelin-1.[40] Platelets may contribute to occlusive neointimal lesions in arterioles and our recent study demonstrating hyperpermeable characteristic of the PAH pulmonary vasculature[34] raises the possibility that platelets could be consumed in the leaky perivascular tissue beds, but further studies elucidating pulmonary and extrapulmonary mechanisms of thrombocytopenia are warranted. Studying PAH-specific pathophysiology involving thrombocytopenia in human populations is particularly challenging, due to the high prevalence of multiple confounding factors including comorbidities known to affect platelet counts, such as liver disease, or medications that can potentially decrease platelet counts in the PAH population, such as anticoagulants.[41,42] To our knowledge, this is the first report of thrombocytopenia as a phenotype of experimental PAH. Considering the normal lab value range for rats is higher than that of humans,[43] and hemoconcentration due to dehydration may be a confounding effect, the severity of thrombocytopenia in our study is profound. This model may help reveal mechanisms involved in development of thrombocytopenia in selected PAH patient populations.

Thayer et al. recently found that RDW portends poor outcomes for non-anemic PAH patients.[9] The value of RDW as a biomarker for multiple cardiovascular diseases has long been suggested,[44,45] but the pathophysiology involved has not been fully elucidated. Interestingly, our PAH rat model developed a non-anemic macrocytic red blood cell phenotype, with increased immature red blood cell production resulting in an increase in RDW. Although hemoglobin was not decreased, it may have been masked by hemoconcentration as discussed above. Since our results indicate actively ongoing concomitant red blood cell loss and production, if we had carried out our study longer, the animals ultimately could have developed iron deficiency.

Anemia and iron deficiency have been reported as poor prognostic markers in pulmonary hypertension. A cohort study of all group pulmonary hypertension demonstrated that hemoglobin levels parallel survival of the patients.[46] Among systemic sclerosis patients, iron deficiency was more prevalent in PAH patients, and among those PAH patients, iron deficiency predicted worse mortality.[47] Our hypoxia-only animal group possessed a hematopoietic response that was characterized by increased red blood cell counts, hemoglobin, hematocrit, MCV, and RDW. Whereas PAH animals showed similarly increased MCV and RDW, their red blood cell counts, hemoglobin, and hematocrit were normal. Furthermore, reticulocyte counts were higher in PAH animals than they were in the control animals, and there was no difference between control and

hypoxia-only groups. This normal reticulocyte count in the hypoxia-only group may be because hypoxia-induced polycythemia is prominent, and additional red blood cell production is not necessary. It remains unclear as to whether increased hemolytic activity contributes to normalization of hematocrit in PAH animals. Overall, we speculate that an increase in red blood cell consumption or destruction related to vasculopathy,[48,49] and an increase in red blood cell production, in part due to the hypoxic hematopoietic response,[50] resulted in macrocytic red blood cell phenotype with high RDW. Since none of hemolytic parameters are highly sensitive or specific as a standalone test, further comprehensive hemolytic workups would be required to confirm hemolytic process in future mechanistic studies.

In conclusion, experimental PAH in Fischer rats reproduces a number of important phenotypes highly relevant to PAH patients. Prior studies highlighted the severe PAH in this animal model, with medial hypertrophy and adventitial thickening, endothelial hyperpermeability, and neo-intimal occlusive lesions, including grades 3, 4, and 6 lesions.[13] Here, we report the animals display biventricular diastolic failure, thrombocytopenia, and red blood cell macrocytosis with high RDW, ultimately predisposing them to sudden death. Our findings emphasize the importance of understanding PAH as a multi-system disease, and, therefore, its therapeutic approach should not be limited to modifying pulmonary vascular and/or right ventricular remodeling. This animal model will be helpful to test and translate therapeutics applicable to selected PAH subpopulations with relevant phenotypes.

Acknowledgements

The authors thank Dr. Gary Ellis Carnahan and Leigh Ann Wiggins for their assistance with blood test analysis and animal anesthesia, respectively.

Author contributions

Conception and design: J.Y.L. and T.S.; data acquisition: J.Y.L., C.Z., and T.S.; analysis and interpretation: J.Y.L., K.A.F., C.Z., L.B., M.V.C., and T.S.; and drafting the manuscript for important intellectual content: J.Y.L. and T.S.

Conflict of interest

The author(s) declare that there is no conflict of interest.

Ethical approval

All animal studies were approved by University of South Alabama IACUC

Funding

This work was supported by 18CDA34080151 (J.Y.L.), HL66299, and HL60024 (T.S.).

ORCID iD

Ji Young Lee https://orcid.org/0000-0002-8005-2446

References

1. Galie N, Humbert M, Vachiery JL, et al. 2015 ESC/ERS guidelines for the diagnosis and treatment of pulmonary hypertension. *Rev Esp Cardiol* 2016; 69: 177.
2. Dweik RA, Rounds S, Erzurum SC, et al. An official American Thoracic Society Statement: pulmonary hypertension phenotypes. *Am J Respir Crit Care Med* 2014; 189: 345–355.
3. Brown LM, Chen H, Halpern S, et al. Delay in recognition of pulmonary arterial hypertension: factors identified from the REVEAL Registry. *Chest* 2011; 140: 19–26.
4. Maron BA and Galiè N. Diagnosis, treatment, and clinical management of pulmonary arterial hypertension in the contemporary era: a review. *JAMA Cardiol* 2016; 1: 1056–1065.
5. D'Alonzo GE, Barst RJ, Ayres SM, et al. Survival in patients with primary pulmonary hypertension. Results from a national prospective registry. *Ann Intern Med* 1991; 115: 343–349.
6. Tonelli AR, Arelli V, Minai OA, et al. Causes and circumstances of death in pulmonary arterial hypertension. *Am J Respir Crit Care Med* 2013; 188: 365–369.
7. Hjalmarsson C, Radegran G, Kylhammar D, et al. Impact of age and comorbidity on risk stratification in idiopathic pulmonary arterial hypertension. *Eur Respir J* 2018; 51: pii1702310.
8. Le RJ, Larsen CM, Fenstad ER, et al. Thrombocytopenia independently predicts death in idiopathic PAH. *Heart Lung* 2019; 48: 34–38.
9. Thayer TE, Huang S, Levinson RT, et al. Unbiased phenome-wide association studies of red cell distribution width identifies key associations with pulmonary hypertension. *Ann Am Thorac Soc* 2019; 16: 589–598.
10. Sztuka K and Jasinska-Stroschein M. Animal models of pulmonary arterial hypertension: a systematic review and meta-analysis of data from 6126 animals. *Pharmacol Res* 2017; 125: 201–214.
11. Abe K, Toba M, Alzoubi A, et al. Formation of plexiform lesions in experimental severe pulmonary arterial hypertension. *Circulation* 2010; 121: 2747–2754.
12. Taraseviciene-Stewart L, Kasahara Y, Alger L, et al. Inhibition of the VEGF receptor 2 combined with chronic hypoxia causes cell death-dependent pulmonary endothelial cell proliferation and severe pulmonary hypertension. *FASEB J* 2001; 15: 427–438.
13. Alzoubi A, Almalouf P, Toba M, et al. TRPC4 inactivation confers a survival benefit in severe pulmonary arterial hypertension. *Am J Pathol* 2013; 183: 1779–1788.
14. Jiang B, Deng Y, Suen C, et al. Marked strain-specific differences in the SU5416 rat model of severe pulmonary arterial hypertension. *Am J Respir Crit Care Med* 2016; 54: 461–468.
15. Francis M, Xu N, Zhou C, et al. Transient receptor potential channel 4 encodes a vascular permeability defect and high-frequency Ca(2+) transients in severe pulmonary arterial hypertension. *Am J Pathol* 2016; 186: 1701–1709.
16. Nagueh SF, Smiseth OA, Appleton CP, et al. Recommendations for the evaluation of left ventricular diastolic function by echocardiography: an update from the American Society of Echocardiography and the European Association of Cardiovascular Imaging. *J Am Soc Echocardiogr* 2016; 29: 277–314.
17. Rudski LG, Lai WW, Afilalo J, et al. Guidelines for the echocardiographic assessment of the right heart in adults: a report

from the American Society of Echocardiography endorsed by the European Association of Echocardiography, a registered branch of the European Society of Cardiology, and the Canadian Society of Echocardiography. *J Am Soc Echocardiogr* 2010; 23: 685–713; quiz 786–688.
18. Quinones MA, Otto CM, Stoddard M, et al. Recommendations for quantification of Doppler echocardiography: a report from the Doppler Quantification Task Force of the Nomenclature and Standards Committee of the American Society of Echocardiography. *J Am Soc Echocardiogr* 2002; 15: 167–184.
19. Zhou C, Townsley MI, Alexeyev M, et al. Endothelial hyperpermeability in severe pulmonary arterial hypertension: role of store-operated calcium entry. *Am J Physiol Lung Cell Mol Physiol* 2016; 311: L560–L569.
20. Naeije R and Manes A. The right ventricle in pulmonary arterial hypertension. *Eur Respir Rev* 2014; 23: 476–487.
21. Hoeper MM and Granton J. Intensive care unit management of patients with severe pulmonary hypertension and right heart failure. *Am J Respir Crit Care Med* 2011; 184: 1114–1124.
22. Santamore WP and Dell'Italia LJ. Ventricular interdependence: significant left ventricular contributions to right ventricular systolic function. *Prog Cardiovasc Dis* 1998; 40: 289–308.
23. De Backer D and Fagnoul D. Intensive care ultrasound: VI. Fluid responsiveness and shock assessment. *Ann Am Thorac Soc* 2014; 11: 129–136.
24. Mojadidi MK, Goodman-Meza D, Eshtehardi P, et al. Thrombocytopenia is an independent predictor of mortality in pulmonary hypertension. *Heart Lung* 2014; 43: 569–573.
25. Rain S, Handoko ML, Trip P, et al. Right ventricular diastolic impairment in patients with pulmonary arterial hypertension. *Circulation* 2013; 128: 2016–2025.
26. Gan CT, Holverda S, Marcus JT, et al. Right ventricular diastolic dysfunction and the acute effects of sildenafil in pulmonary hypertension patients. *Chest* 2007; 132: 11–17.
27. Neto-Neves EM, Frump AL, Vayl A, et al. Isolated heart model demonstrates evidence of contractile and diastolic dysfunction in right ventricles from rats with sugen/hypoxia-induced pulmonary hypertension. *Physiol Rep* 2017; 5: pii: e13438.
28. Tonelli AR, Plana JC, Heresi GA, et al. Prevalence and prognostic value of left ventricular diastolic dysfunction in idiopathic and heritable pulmonary arterial hypertension. *CHEST* 2012; 141: 1457–1465.
29. Hardegree EL, Sachdev A, Fenstad ER, et al. Impaired left ventricular mechanics in pulmonary arterial hypertension: identification of a cohort at high risk. *Circ Heart Fail* 2013; 6: 748–755.
30. Nelson GS, Sayed-Ahmed EY, Kroeker CA, et al. Compression of interventricular septum during right ventricular pressure loading. *Am J Physiol Heart Circ Physiol* 2001; 280: H2639–H2648.
31. Manders E, Bogaard HJ, Handoko ML, et al. Contractile dysfunction of left ventricular cardiomyocytes in patients with pulmonary arterial hypertension. *J Am Coll Cardiol* 2014; 64: 28–37.
32. Kasner M, Westermann D, Steendijk P, et al. Left ventricular dysfunction induced by nonsevere idiopathic pulmonary arterial hypertension: a pressure-volume relationship study. *Am J Respir Crit Care Med* 2012; 186: 181–189.
33. Fayyaz AU, Edwards WD, Maleszewski JJ, et al. Global pulmonary vascular remodeling in pulmonary hypertension associated with heart failure and preserved or reduced ejection fraction. *Circulation* 2018; 137: 1796–1810.
34. Zhou C, Crockett ES, Batten L, et al. Pulmonary vascular dysfunction secondary to pulmonary arterial hypertension: insights gained through retrograde perfusion. *Am J Physiol Lung Cell Mol Physiol* 2018; 314: L835–L845.
35. Stumpe KO, Solle H, Klein H, et al. Mechanism of sodium and water retention in rats with experimental heart failure. *Kidney Int* 1973; 4: 309–317.
36. Nielsen S, Terris J, Andersen D, et al. Congestive heart failure in rats is associated with increased expression and targeting of aquaporin-2 water channel in collecting duct. *Proc Natl Acad Sci U S A* 1997; 94: 5450–5455.
37. Kalantari K, Chang JN, Ronco C, et al. Assessment of intravascular volume status and volume responsiveness in critically ill patients. *Kidney Int* 2013; 83: 1017–1028.
38. Varol E, Uysal BA and Ozaydin M. Platelet indices in patients with pulmonary arterial hypertension. *Clin Appl Thromb Hemost* 2011; 17: E171–E174.
39. Zanjani KS. Platelets in pulmonary hypertension: a causative role or a simple association? *Iran J Pediatr* 2012; 22: 145–157.
40. Budhiraja R, Tuder RM and Hassoun PM. Endothelial dysfunction in pulmonary hypertension. *Circulation* 2004; 109: 159–165.
41. Chin KM, Channick RN, de Lemos JA, et al. Hemodynamics and epoprostenol use are associated with thrombocytopenia in pulmonary arterial hypertension. *Chest* 2009; 135: 130–136.
42. Khan MS, Usman MS, Siddiqi TJ, et al. Is anticoagulation beneficial in pulmonary arterial hypertension? *Circ Cardiovasc Qual Outcomes* 2018; 11: e004757.
43. He Q, Su G, Liu K, et al. Sex-specific reference intervals of hematologic and biochemical analytes in Sprague-Dawley rats using the nonparametric rank percentile method. *PLoS One* 2017; 12: e0189837.
44. Danese E, Lippi G and Montagnana M. Red blood cell distribution width and cardiovascular diseases. *J Thorac Dis* 2015; 7: E402–E411.
45. Smukowska-Gorynia A, Tomaszewska I, Malaczynska-Rajpold K, et al. Red blood cells distribution width as a potential prognostic biomarker in patients with pulmonary arterial hypertension and chronic thromboembolic pulmonary hypertension. *Heart Lung* 2018; 27: 842–848.
46. Krasuski RA, Hart SA, Smith B, et al. Association of anemia and long-term survival in patients with pulmonary hypertension. *Int J Cardiol* 2011; 150: 291–295.
47. Ruiter G, Lanser IJ, de Man FS, et al. Iron deficiency in systemic sclerosis patients with and without pulmonary hypertension. *Rheumatology (Oxford, England)* 2014; 53: 285–292.
48. Jubelirer SJ. Primary pulmonary hypertension. Its association with microangiopathic hemolytic anemia and thrombocytopenia. *Arch Intern Med* 1991; 151: 1221–1223.
49. Machado RF and Farber HW. Pulmonary hypertension associated with chronic hemolytic anemia and other blood disorders. *Clin Chest Med* 2013; 34: 739–752.
50. Tsantes AE, Papadhimitriou SI, Tassiopoulos ST, et al. Red cell macrocytosis in hypoxemic patients with chronic obstructive pulmonary disease. *Respir Med* 2004; 98: 1117–1123.